Motile sperm domain containing 1 is upregulated by the Wnt/β-catenin signaling pathway in colorectal cancer

CHIAKI HORIE[1*], CHI ZHU[1*], KIYOSHI YAMAGUCHI[1], SAYA NAKAGAWA[1], YUMIKO ISOBE[1], KIYOKO TAKANE[1], TSUNEO IKENOUE[1], YASUNORI OHTA[2], YUKIHISA TANAKA[2], SUSUMU AIKOU[3], GIICHIRO TSURITA[3], YUKA AHIKO[3], DAI SHIDA[3] and YOICHI FURUKAWA[1]

[1]Division of Clinical Genome Research, Advanced Clinical Research Center, Institute of Medical Science, The University of Tokyo; Departments of [2]Pathology and [3]Surgery, Research Hospital, Institute of Medical Science, The University of Tokyo, Tokyo 108-8639, Japan

Received February 28, 2022; Accepted May 17, 2022

DOI: 10.3892/ol.2022.13402

Abstract. Aberrant activation of the Wnt/β-catenin signaling pathway plays a crucial role in the development and progression of colorectal cancer. Previously, we identified a set of candidate genes that were regulated by this signaling pathway, and the present study focused on motile sperm domain containing 1 (*MOSPD1*). Immunohistochemical staining revealed that the expression of MOSPD1 was elevated in tumor cells from colorectal cancer tissues compared with in non-tumor cells. Using ChIP-seq data and the JASPAR database, the regulatory region(s) in the *MOSPD1* gene as a target of the Wnt/β-catenin signaling pathway were searched, and a region containing three putative TCF-binding motifs in the 3'-flanking region was identified. Additional analyses using reporter assay and ChIP-quantitative PCR suggested that this region harbors enhancer activity through an interaction with transcription factor 7 like 2 (TCF7L2) and β-catenin. In addition, chromatin conformation capture assay revealed that the 3'-flanking region interacts with the *MOSPD1* promoter. These data suggested that *MOSPD1* was regulated by the β-catenin/TCF7L2 complex through the enhancer element located in the 3'-flanking region. These findings may be helpful for future studies regarding the precise regulatory mechanisms of MOSPD1.

Correspondence to: Dr Kiyoshi Yamaguchi, Division of Clinical Genome Research, Advanced Clinical Research Center, Institute of Medical Science, The University of Tokyo, 4-6-1 Shirokanedai, Minato-ku, Tokyo 108-8639, Japan
E-mail: kiyamagu@g.ecc.u-tokyo.ac.jp

*Contributed equally

Key words: motile sperm domain containing 1, Wnt, β-catenin, transcription factor 7 like 2, colorectal cancer

Introduction

The Wnt/β-catenin signaling pathway (also known as the canonical Wnt pathway) is responsible for embryonic development and tissue homeostasis (1). Aberrant activation of this pathway by genetic and epigenetic alterations is involved in human diseases such as cancer (2-4). In colorectal cancer (CRC), frequent activation of Wnt/β-catenin signaling pathway by somatic mutations in APC regulator of WNT signaling pathway (*APC*) or the β-catenin gene (*CTNNB1*) has been reported. In the cBioPortal for Cancer Genomics (https://www.cbioportal.org/), a public database of cancer genomes, mutations of *APC* and *CTNNB1* were found in 64 and 6%, respectively, of 3,051 CRC tissues. Loss of function mutations in *APC* or activating mutations in *CTNNB1* result in the stabilization and accumulation of β-catenin protein in the cells. The accumulated β-catenin interacts with T cell factor (TCF)/lymphoid enhancer-binding factor (LEF) transcription factors in the nucleus, and induces the expression of their target genes (Wnt target genes) (5). To date, more than one hundred Wnt target genes have been identified, and a list of the genes is shown on the Wnt homepage at https://web.stanford.edu/group/nusselab/cgi-bin/wnt/target_genes. Studies of their function have helped to further understand the molecular mechanisms of carcinogenesis and the complex regulatory mechanisms underlying this signaling pathway. Representative examples of the aberrant activation of this pathway contributing to carcinogenesis include MYC proto-oncogene (*MYC*) and cyclin D1 (*CCND1*). *MYC* was identified by serial analysis of gene expression using HT29 cells containing a zinc-inducible APC, and affects a wide variety of functions such as cell proliferation, angiogenesis, and promotion of anaerobic metabolism (6). *Cyclin D1* is known to regulate G1-S cell cycle progression, and it was identified through the analysis of human genes involved in controlling cell growth, the promoter regions of which contain the core TCF/LEF-binding sites (7).

It is of note that chromatin immunoprecipitation coupled with high-throughput sequencing (ChIP-seq) analysis using six different cell lines and anti-TCF7L2 antibody identified 116,000 non-redundant TCF7L2-binding sites, with 1,864 sites common to the cell lines tested, suggesting the existence

of as yet unidentified Wnt target genes in human cells (8). To understand the precise molecular mechanism underlying the development of Wnt-driven cancer, we previously searched for new target genes by microarray using β-catenin-depleted CRC cells and ChIP-seq of TCF7L2. Integrated analysis of these data identified 11 candidate genes that are directly regulated by the β-catenin/TCF7L2 complex (9). Among these candidates, we focused in this study on motile sperm domain containing 1 (*MOSPD1*), and revealed that *MOSPD1* is a novel direct target of the Wnt signaling pathway. Furthermore, we identified three Wnt responsive elements in the 3'-flanking region of *MOSPD1*, and showed that the elements are involved in the transcriptional activation. These data will help deepen our understanding of colorectal carcinogenesis, as well as the regulatory mechanism of MOSPD1.

Materials and methods

Cell culture. Human CRC cell lines, HCT116 (CCL-247) and SW480 (CCL-228), and a human endocervical adenocarcinoma cell line, HeLa (CCL-2) were purchased from the American Type Culture Collection. All cell lines were grown in appropriate media (McCoy's 5a Modified Medium for HCT116, Leibovitz's L-15 Medium for SW480, and Eagle's Minimum Essential Medium for HeLa) supplemented with 10% fetal bovine serum (BioSera), and antibiotic/antimycotic solution (Fujifilm Wako Pure Chemical). HCT116 and HeLa cells were maintained in 5% CO_2 at 37˚C, and SW480 cells were maintained without CO_2 supplementation at 37˚C.

Reporter plasmids and luciferase assay. Two genomic regions of 5'-putative (GRCh38-chrX: 134,932,384-134,933,013) and 3'-putative enhancers (GRCh38-chrX: 134,885,255-134,886,704) were amplified by PCR using region-specific primer sets and genomic DNA extracted from the peripheral blood of healthy volunteers as a template. After digestion with *Xho*I and *Bgl*II restriction enzymes, the PCR products were cloned into pGL4.23 vector (Promega) to generate pGL4.23-MOSPD1-5'E and pGL4.23-MOSPD1-3'E. The primer sequences are shown in Table SI. Construction of pCAGGS-dominant negative TCF7L2 (dnTCF7L2) was described previously (10). Significant suppression of β-catenin/TCF-dependent transcriptional activity using pCAGGS-dnTCF7L2 has been confirmed in the previous studies (11-13). HCT116 cells were transfected with these reporter plasmids together with β-catenin siRNAs or pCAGGS-dnTCF7L2 using Lipofectamine 2000 (Thermo Fisher Scientific). pRL-null plasmids were co-transfected with the reporter plasmids for normalization. 48 h after the transfection, the cells were lysed and reporter activities were measured using dual luciferase kit (TOYO B-Net) and Lumat LB9507 Luminometer (Berthold Technologies). Firefly luciferase activity was normalized to *Renilla* luciferase activity (pRL-null).

Site-directed mutagenesis. TCF-binding motifs were searched by JASPAR, a database for transcription factor binding profiles (14). Mutant reporter plasmids containing substitutions in the consensus sequence of the TCF-binding motifs were prepared by site-directed mutagenesis. Wild type-plasmid DNA of pGL4.23-MOSPD1-3'E was amplified using KOD-Plus-Neo (Toyobo) and a set of mutagenic primers (Table SII). The PCR products were digested with *Dpn*I restriction enzyme (Takara Bio) to cleave the methylated template DNA, followed by transformation into *Escherichia coli*. Insertion of mutations in the plasmids was confirmed by Sanger sequencing (data not shown; 3500xl DNA Analyzer; Thermo Fisher Scientific).

Gene silencing. For the knockdown of β-catenin, two β-catenin siRNAs (siβ-catenin#9: 5'-GAUCCUAGCUAUCGUUCUU-3' and siβ-catenin#10: 5'-UAAUGAGGACCUAUACUUA-3'; Merck) were used. Control siRNA (siControl, ON-TARGET plus non-targeting Pool, #D-001810-10-20) was purchased from Horizon Discovery. Cells were transfected with 10 nM of the indicated siRNA using Lipofectamine RNAiMAX or Lipofectamine 2000 (Thermo Fisher Scientific) for 48 h.

Western blotting. Total protein was extracted from cultured cells using SDS sample buffer (25 mM Tris-HCl, pH 6.8, 0.8% sodium dodecyl sulfate, 4% glycerol). After boiling the samples for 10 min, the protein was separated by SDS-PAGE, and transferred onto a nitrocellulose membrane (GE Healthcare). The membranes were blocked with 5% milk in TBS-T (Tris-buffered saline-Tween-20), and then incubated with primary antibody; anti-MOSPD1 (GTX32111; GeneTex), anti-β-catenin (9582; Cell Signaling Technology), or anti-β-actin (A5441; Merck). Horseradish peroxidase-conjugated goat anti-mouse or anti-rabbit IgG (GE Healthcare) served as the secondary antibody for the ECL Detection System (GE Healthcare).

Chromatin immunoprecipitation assay. Chromatin immunoprecipitation followed by qPCR (ChIP-qPCR) was performed as described previously (15). Briefly, HCT116 cells were cross-linked with 1% formaldehyde for 10 min at room temperature, and 0.1 M glycine was added to quench the formaldehyde. Chromatin was extracted and sheared by micrococcal nuclease digestion (New England Biolabs). Subsequently, protein-DNA complexes were immunoprecipitated with 10 μg of anti-TCF7L2 antibody (05-511; Merck) bound to Dynabeads Protein G (Thermo Fisher Scientific). Normal mouse IgG (Santa Cruz Biotechnology) was used as a negative control. The precipitated protein-DNA complexes were purified by conventional DNA extraction methods, and the purified DNA was subjected to qPCR analysis using KAPA SYBR FAST ABI prism Kit (Kapa Biosystems) and a set of primers encompassing the TCF-binding motifs located in the 3'-flanking region of *MOSPD1*. Amplification of a region upstream of the *GAPDH* gene was used as a negative control. Sequences of the primers are shown in Table SIII.

Chromatin conformation capture (3C) assay. 3C was performed as described previously, with minor modifications (16). Briefly, SW480 cells were cross-linked with 1% formaldehyde for 10 min at room temperature, and then treated with 0.125 M glycine. The cross-linked chromatin was digested at 37˚C overnight with 400 units of *Hin*dIII (Takara Bio), and subsequently heat-inactivated for 25 min at 65˚C in the presence of SDS (1.6%) prior to ligation. DNA

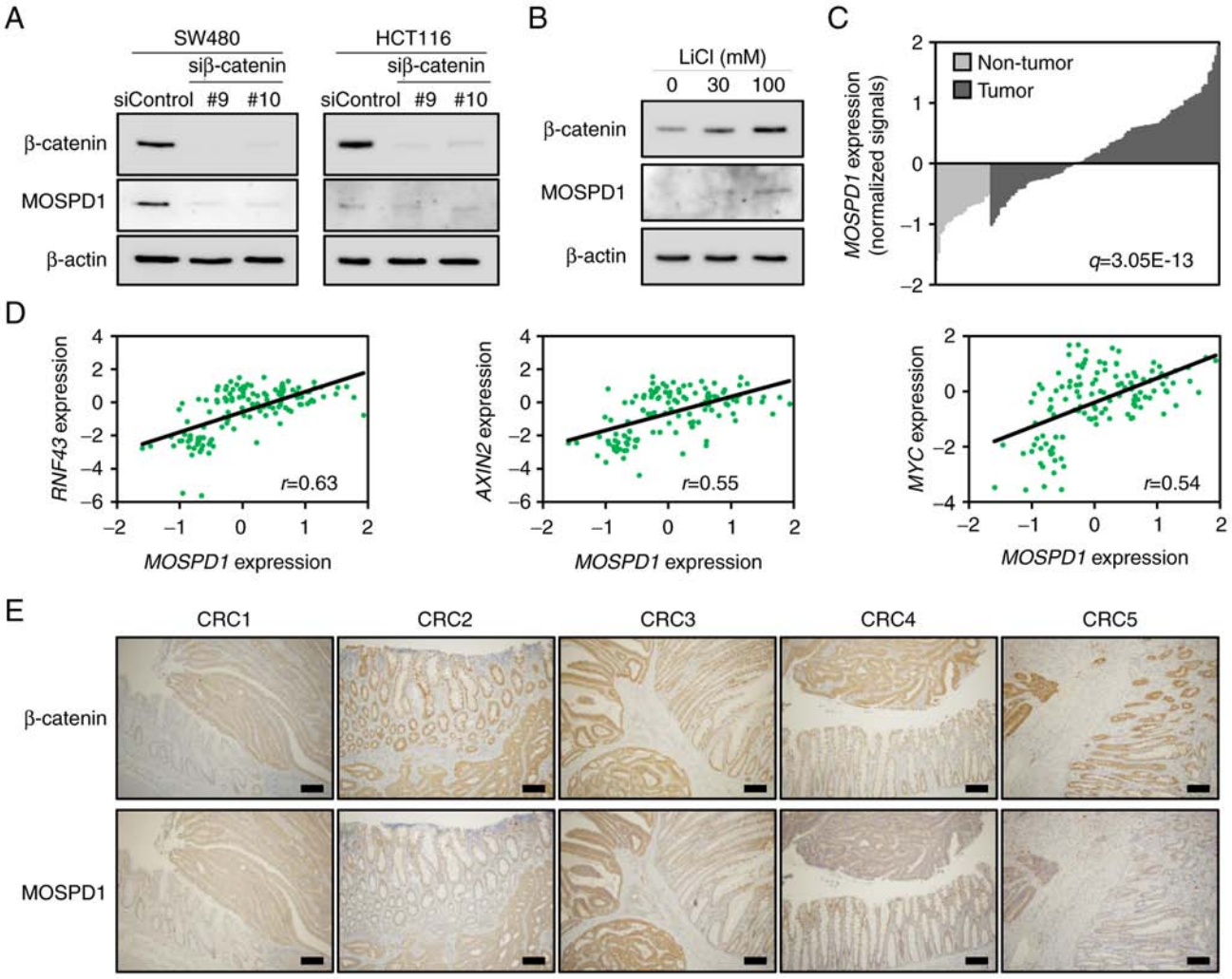

Figure 1. MOSPD1 is regulated by the Wnt/β-catenin signaling in colorectal cancer. (A) Suppressed expression of MOSPD1 by β-catenin siRNAs in SW480 and HCT116 cells. (B) Induction of β-catenin in HeLa cells treated with LiCl (30 and 100 mM) increased MOSPD1 expression. The expression of β-actin served as a loading control. (C) Expression of *MOSPD1* in 104 CRC tissues and 25 non-tumorous colonic tissues. The data were obtained from a dataset of GSE21510 in GEO. Statistical significance was determined by unpaired t-test with Benjamini-Hochberg correction. (D) The Pearson's correlation coefficient (*r*) between the expression values of *MOSPD1* and three Wnt target genes was calculated to assess their correlation. The solid line indicates linear fit. The data were obtained from GSE21510. (E) Immunohistochemical staining of β-catenin (upper) and MOSPD1 (lower) in CRC tissues. Scale bars 200 μm. MOSPD1, motile sperm domain containing 1; LiCl, lithium chloride; CRC, colorectal cancer; GEO, Gene Expression Omnibus.

fragments were ligated with 2,000 U of T4 DNA ligase (New England Biolabs) for 8 h at 16˚C. Samples were treated with Proteinase K (300 μg; Merck) at 37˚C overnight to reverse the cross-links. After treatment with RNase A (300 μg; Merck), the DNA was purified by phenol/chloroform extraction and ethanol precipitation. Nested PCR (KOD One, Toyobo) was performed to investigate a possible interaction between the promoter and enhancer regions of *MOSPD1*. The sequences of 1st and nested primers are shown in Table SIV.

Immunohistochemical staining. All colorectal tumor tissues and corresponding non-cancerous tissues were obtained with written informed consent from resected specimens of 11 patients who underwent surgery. The clinical and histological information of the 11 CRCs is shown in Supplementary Table SV. Tissue sections were deparaffinized with xylene and rehydrated in a graded series of ethanol. Antigen retrieval was performed using 0.01 M citrate buffer (pH 6.0) and autoclave heating at 110˚C for 10 min. After blocking endogenous peroxidase activity in 0.3% H_2O_2 (Fujifilm Wako Pure Chemical) for 5 min, slides were incubated with 5% goat serum (ab7481; Abcam) for 8 min, followed by the incubation with anti-MOSPD1 (GeneTex, 1:200) or anti-β-catenin antibody (RB-1491; NeoMarkers, 1:300) at 4˚C overnight. Secondary antibody, Dako EnVision™+ Dual Link System-HRP (Dako), and ImmPACT DAB Substrate Kit (Vecter Laboratories) were then used to visualize the immunoreactivity. Tissue sections were counterstained with hematoxylin (Merck).

Statistical analysis. Gene expression values of human colorectal tumors (GSE21510) (17) were obtained from the Gene Expression Omnibus (https://www.ncbi.nlm.nih.gov/geo/). An unpaired t-test with Benjamini-Hochberg correction was applied to evaluate the differential expression of *MOSPD1* between 104 tumors and 25 matched non-cancerous controls. Correlation between the expression values of *MOSPD1* and known Wnt target genes was determined using Pearson's correlation coefficient (*r*). Experiments

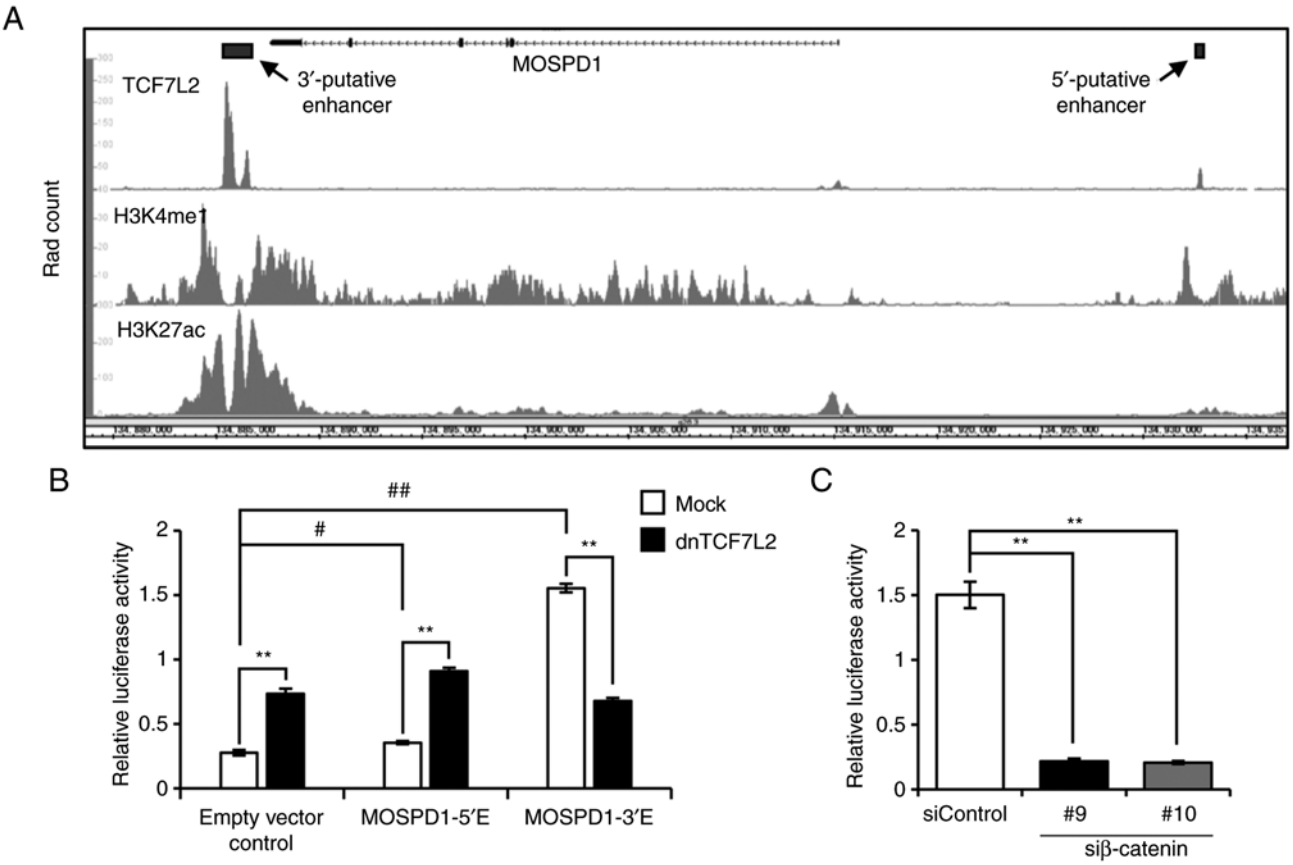

Figure 2. TCF7L2-interacting region in the 3'-flanking region may play a role as an enhancer. (A) Schematic representation of the ENCODE ChIP-seq data of TCF7L2 (ENCSR000EUV), H3K4me1 (ENCSR161MXP), and H3K27ac (ENCSR000EUT) in HCT116 cells. (B) Reporter activity of putative enhancer regions in the 5'- and 3'-flanking regions. HCT116 cells were transfected with pGL4.23 (Empty vector control), pGL4.23-MOSPD1-5'E (MOSPD1-5'E), or pGL4.23-MOSPD1-3'E (MOSPD1-3'E) plasmids, in combination with pRL-null reporter plasmids for the normalization of transfection. The cells were co-transfected with pCAGGS-dnTCF7L2 plasmids expressing a dominant-negative form of TCF7L2 or the empty plasmids (Mock). Relative luciferase activities represent mean ± SD from three independent cultures. Statistical significance was determined by one-way ANOVA, followed by Turkey's test; **P<0.01, as compared with Mock; $^{\#}$P<0.05, $^{\#\#}$P<0.01, as compared with Empty vector control. (C) Effect of β-catenin siRNA on the reporter activity of MOSPD1-3'E in HCT116 cells. Relative luciferase activities represent mean ± SD from three independent cultures. Statistical significance was determined by one-way ANOVA, followed by Dunnett's test; **P<0.01, as compared with siControl. TCF7L2, transcription factor 7 like 2; ENCODE, The Encyclopedia of DNA Elements; ChIP, chromatin immunoprecipitation; MOSPD1, motile sperm domain containing 1; H3K4me1, histone H3 lysine 4 mono-methylation; H3K27ac, histone H3 lysine 27 acetylation.

were performed in biological triplicate and data are presented as the mean ± standard deviation (SD). To compare the means between two groups in ChIP-qPCR, the unpaired t-test was used. Statistical analysis of data from reporter assays was performed using one-way analysis of variance (ANOVA) followed by Tukey's or Dunnett's multiple comparisons test. We used the BellCurve for Excel software for the analyses (Social Survey Research Information). P<0.05 was considered to indicate a statistically significant difference.

Results

The expression of MOSPD1 is regulated by Wnt/β-catenin signaling in colorectal cancer cells. In the previous study, we identified a total of 11 target genes whose expression was commonly down-regulated by the introduction of β-catenin siRNAs and a dominant-negative form of TCF7L2 (dnTCF7L2) in HCT116, SW480, and LS174T cells (9). Subsequent qPCR analysis revealed that the expression of *PDE4D*, *PHLDB2*, *OXR1*, *FRMD5*, and *MOSPD1* was significantly decreased by the knockdown of β-catenin. To verify the association of MOSPD1 with the Wnt/β-catenin signaling, we performed western blot analysis using lysates from SW480 and HCT116 cells treated with β-catenin or control siRNA. In agreement with the qPCR data, treatment with two independent β-catenin siRNAs decreased MOSPD1 expression in both cells (Fig. 1A). In addition, treatment of HeLa cells with lithium chloride (LiCl), a glycogen synthase kinase 3 (GSK3) inhibitor that activates the Wnt/β-catenin signaling, increased β-catenin and MOSPD1 expression (Fig. 1B). These data corroborated that MOSPD1 is a downstream target of the Wnt/β-catenin signaling.

Since aberrant activation of the Wnt/β-catenin signaling is involved in the majority of CRC (2,18), we searched for gene expression data of colorectal tumors in NCBI Gene Expression Omnibus. In a dataset (GSE21510) containing 104 CRC tissues and 25 non-tumorous colonic tissues (17), the average *MOSPD1* expression was found to be 2.18-fold higher (q-value: 3.05E-13) in the tumor tissues than in the non-tumorous tissues (Fig. 1C). In addition, the expression levels showed a tendency of positive correlation with *RNF43* (r=0.63), *AXIN2* (r=0.55), and *MYC* (r=0.54), three well-known Wnt targets (Fig. 1D).

These data supported that *MOSPD1* expression is induced by the activation of Wnt signaling.

We further carried out immunohistochemical staining of β-catenin and MOSPD1 using 11 CRC tissues. As shown in Fig. 1E, β-catenin was stained in the cytoplasm and/or nucleus of tumorous cells in all tumor tissues tested. MOSPD1 was positively stained in tumor lesions of all CRC cases tested. In addition, MOSPD1 was also positively stained in the cytoplasm and/or nucleus of the tumorous cells (Fig. 1E, lower paned).

Identification of an enhancer in the 3'-flanking region of MOSPD1. In our previous study, ChIP-seq analysis showed a region for the binding with TCF7L2 in the 3'-flaking region of *MOSPD1* (3'-putative enhancer, GRCh 38-chrX:134,885,306-134,886,672) (9). This region was overlapped with a peak in ENCODE ChIP-seq data of TCF7L2 (ENCSR000EUV, Fig. 2A, upper panel). In addition to the 3'-region, the ENCODE data showed another peak in the 5'-flanking region of *MOSPD1* (GRCh38-chrX: 134,932,561-134,932,930). These peaks were overlapped with peaks of histone modifications (H3K4me1: ENCSR161MXP and H3K27Ac: ENCSR000EUT, Fig. 2A, middle and lower panels), suggesting that these regions may have enhancer activity through the interaction with TCF7L2. To investigate their enhancer activity, these regions were cloned into reporter plasmids, and reporter assays were performed using HCT116 cells. As a result, both reporter plasmids, pGL4.23-MOSPD1-5'E and pGL4.23-MOSPD1-3'E, showed increased reporter activity compared to the mock reporter (empty vector control) by 1.29- and 5.62-fold, respectively (Fig. 2B). Importantly, co-transfection of the reporter plasmids with plasmids expressing dnTCF7L2 significantly decreased the reporter activity of pGL4.23-MOSPD1-3'E, but not the activity of pGL4.23-MOSPD1-5'E, suggesting the enhancer activity of the 3'-flanking region through the interaction with TCF7L2. In addition, knockdown of β-catenin by two independent siRNAs markedly reduced the reporter activity of pGL4.23-MOSPD1-3'E (Fig. 2C).

Involvement of three TCF-binding motifs in the enhancer activity. We further searched for TCF-binding elements (TBE) in the 3'-enhancer region using JASPAR, a database for transcription factor binding profiles (14), and identified eight candidate TBEs (Table SVI). Among the eight, we focused on three TBEs with a similarity score greater than 10; TBE1 (GRCh38-chrX: 134,885,716-134,885,729), TBE2 (GRCh38-chrX: 134,885,543-134,885,556), and TBE3 (GRCh38-chrX: 134,885,482-134,885,495). To investigate the involvement of these motifs in the enhancer activity, we prepared mutant reporter plasmids containing two-nucleotide substitutions in each TCF-binding motif (TBE1-mut, TBE2-mut, and TBE3-mut) of pGL4.23-MOSPD1-3'E and reporter plasmids containing these substitutions in the three motifs (TBEall-mut) (Fig. 3A). A reporter assay determined that the reporter activity of mutant plasmids (TBE1-mut, TBE2-mut, and TBE3-mut) was significantly reduced compared to the wild type plasmids (pGL4.23-MOSPD1-3'E) by 9.87, 35.3, and 35.0%, respectively. In addition, the activity of TBEall-mut plasmids was markedly decreased compared to the wild type by 85.6% (Fig. 3B). Treatment of

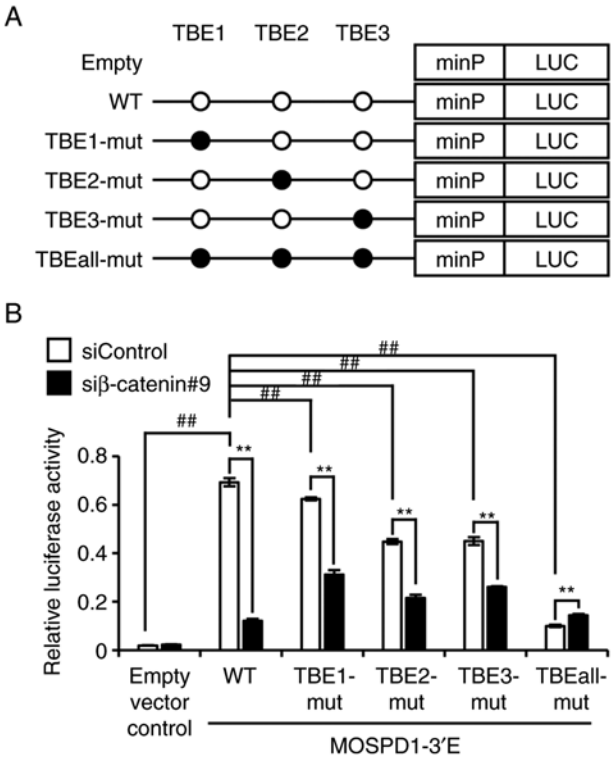

Figure 3. Involvement of the three TBEs in the reporter activity. (A) Schematic representation of wild type (open circle: WWCAAAG, W: A/T) and mutant (closed circle: WWCAGCG) TCF-binding motifs in pGL4.23-MOSPD1-3'E reporter plasmids. (B) Relative reporter activity of empty, wild type and mutant reporter plasmids in HCT116 cells (Empty vector control, WT, TBE1-mut, TBE2-mut, TBE3-mut, or TBEall-mut). The data represent mean ± SD from three independent cultures. Statistical significance was determined by one-way ANOVA, followed by Turkey's test; **P<0.01, as compared with siControl; $^{\#\#}$P<0.01, as compared with pGL4.23-MOSPD1-3'E WT. TBEs, TCF-binding elements; WT, wild type; MOSPD1, motile sperm domain containing 1.

the cells expressing TBE1-mut, TBE2-mut, or TBE3-mut with β-catenin siRNA suppressed the activity by 50.2, 52.2, and 42.3%, respectively, compared to the cells with control siRNA. These data indicated that the three motifs are, at least in part, associated with the enhancer activity of TCF7L2.

Identification of the interaction between 3'-putative enhancer and promoter region of MOSPD1. To confirm the interaction between the 3'-flanking region of *MOSPD1* and TCF7L2, we performed a ChIP-qPCR assay using anti-TCF7L2 antibody and region-specific primer sets for the 3'-enhancer region of *MOSPD1*. An enhancer region in intron 2 of *RNF43* was recruited as a positive control (19). This assay detected an enrichment of the enhancer region in *RNF43* by 4.53-fold in the precipitants with the anti-TCF7L2 antibody compared to those with normal IgG. DNA fragments containing the 3'-enhancer region of *MOSPD1* were enriched by 10.3-fold in the precipitants (Fig. 4A).

To investigate whether the distal 3'-putative enhancer region interacts with the promoter region of *MOSPD1*, we performed a 3C assay. We used DNA from SW480 cells after the fixation with formaldehyde and subsequent digestion with a restriction enzyme *Hin*dIII. Self-ligation of the DNA was expected to produce six types of chromatin loops when the

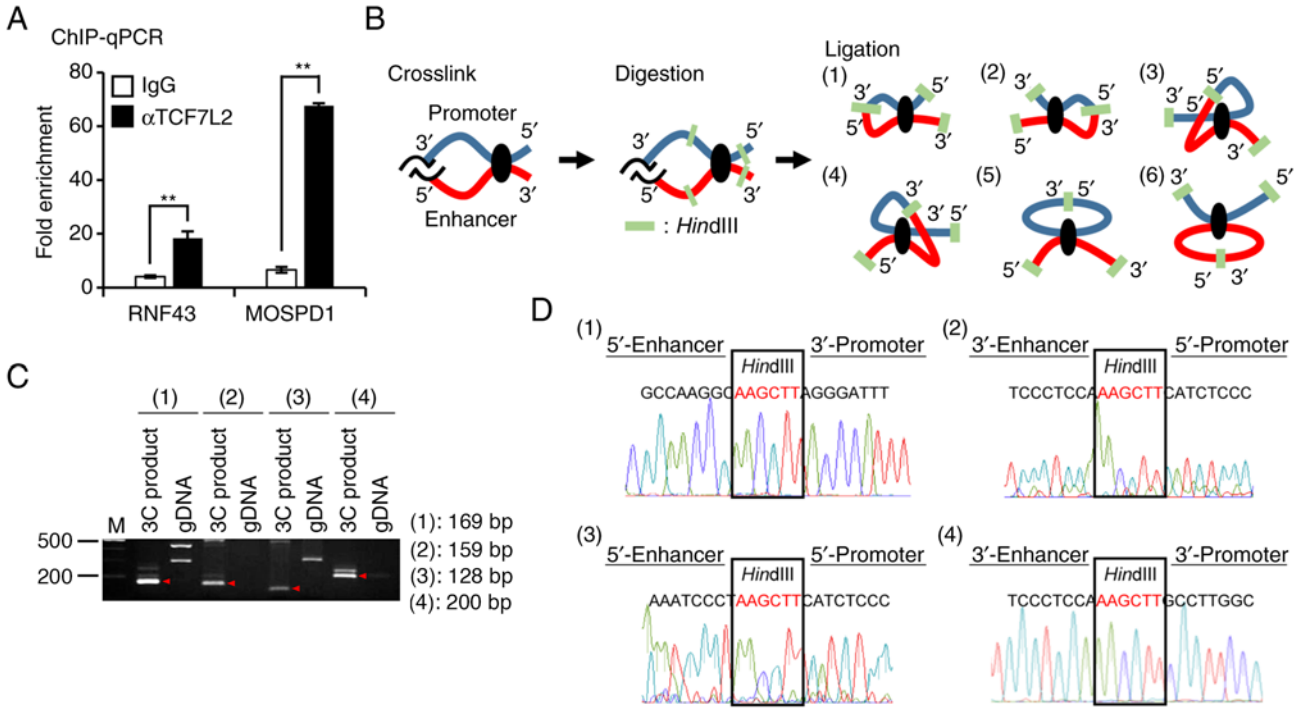

Figure 4. The interaction between the enhancer and promoter regions of *MOSPD1*. (A) ChIP-qPCR was performed using region-specific primer sets and the precipitants with an anti-TCF7L2 antibody or those with normal IgG. The amplification of a region upstream of *GAPDH* was used for normalization. The enhancer region in intron 2 of *RNF43* was used as a positive control. Data represents mean ± SD from three independent experiments. A significant difference was determined by unpaired Student's t-test: $^{**}P<0.01$. (B) Schematic representation of expected chromatin loops in the 3C product. (C) An image of gel electrophoresis of the PCR products. The 3C product was amplified using four sets of 1st and nested PCR primers. Genomic DNA (gDNA) extracted from SW480 cells was used as a negative control. (D) The sequence electropherogram of the PCR products. MOSPD1, motile sperm domain containing 1; ChIP, chromatin immunoprecipitation; GAPDH, glyceraldehyde-3-phosphate dehydrogenase; RNF43, ring finger protein 43; 3C, chromatin conformation capture.

two regions were closely associated (Fig. 4B). We designed four sets of 1st and nested primers that can detect the associations between the promoter and enhancer regions (Table SIV). As a result, amplification of the DNA with the four primer sets detected PCR products with the expected size, but it failed to amplify control DNA extracted from SW480 cells (Fig. 4C). Additional sequence analysis of the PCR products confirmed the interactions of enhancer-promoter regions connected with a *Hin*dIII restriction enzyme site (Fig. 4D). These data suggested that the distal enhancer located in the 3'-flanking region interacts with the promoter region through the formation of a chromatin loop.

Discussion

In this study, we revealed that *MOSPD1* is transcriptionally regulated by Wnt signaling through the three TBEs located in its 3'-flanking region.

MOSPD1 is a member of major sperm protein (MSP) domain-containing family that is highly conserved in many species. There are three MSP domain-containing proteins (MOSPD1, 2, and 3) in humans, and four (Mospd1, 2, 3, and 4) in mice and rats (20). The similarities between human MOSPD1 and human MOSPD2, and that between human MOSPD1 and human MOSPD3 are 8 and 32%, respectively, at protein levels (CLUSTALW, https://www.genome.jp/tools-bin/clustalw). In our previous expression profile analysis, knockdown of β-catenin did not show significant decrease of *MOSPD2* or *MOSPD3* in SW480 cells. These data may imply that MOSPD1 has a specific function that is linked with the canonical Wnt signaling pathway in development.

The function of MOSPD1 is still largely unclarified. In the early 1980s, MSP was isolated as a protein 15K from sperm cells of *Caenorhabditis elegans* (21), implying its role in spermatogenesis. Later, MSP was shown to function as a motility apparatus in sperm locomotion (22,23). In GTEx Portal, a public database of gene expression in normal tissues (https://gtexportal.org/home/), *MOSPD1* is expressed in a variety of tissues including esophageal mucosa, adrenal gland, testis, skin, and uterus, suggesting that MOSPD1 should play physiological role(s) in various tissues. In mice, *Mospd1* is abundantly expressed in mesenchymal tissues, and its expression is elevated during differentiation in osteoblastic, myoblastic, and adipocytic cell lines (20). Another study revealed that Mospd1-null embryonic stem cells were able to proliferate and that they were unable to differentiate to osteoblasts, adipocytes, and hematopoietic progenitors (24). These data indicated that Mospd1 should be involved in the differentiation and proliferation of mesenchymal cells. In addition, knockdown of *Mospd1* induced the expression of epithelial cadherin *Cdh1*, and decreased the expression of *Snai1*, *Snai2*, and mesenchymal cadherin *Cdh11* in MC3T3-E1 cells established from mouse osteoblasts (20). These results suggested that Mospd1 may be associated with epithelial-mesenchymal transition (EMT). EMT plays an important role in the invasion or metastasis of cancer. Ovarian cancer cells with high invasion-phenotype expressed significantly increased levels of MOSPD1 compared to the cells with low invasion-phenotype (25). Besides, the activation of Wnt signaling pathway lead to induce EMT in cancer (26).

Thus, further functional analysis of MOSPD1 in EMT may give us better understanding of the EMT-induction mechanism by Wnt signaling pathway. Interestingly, expression of *Runx2* and *Osteocalcin* was also down-regulated by the knockdown of *Mospd1* in MC3T3-E1 cells (20). RUNX2, one of the transcription factors required for osteoblastic differentiation is abundantly expressed in the nucleus of osteoid osteoma cells (27). It is noteworthy that osteomas frequently develop in the mandible bone of patients with germline variants in the *APC* gene (28). The induction of RUNX2 and/or osteocalcin by the increased expression of MOSPD1 in osteoblasts may be involved in the development of osteomas in patients with familial polyposis of the colon.

We identified a distant enhancer region for the Wnt/β-catenin signaling in the 3'-flanking region of *MOSPD1*. Enhancer regions that associate with β-catenin-TCF/LEF1 complexes have been identified in various regions of the target genes. For instance, the enhancer regions of *MYC* (6), *CCND1* (7), claudin-1 (*CLDN1*) (11), membrane-type matrix metalloproteinase (*MT1-MMP*) (12), and *SP5* (29) are localized in their 5'-flanking regions, and those of *RNF43* (19) and *FRMD5* (9) in intron 2 and intron 1, respectively. Regarding *AXIN2*, several enhancer regions have been discovered in its 5'-flanking region and in intron 1 (30). It is of note that, in addition to the 5'-flanking enhancer region, *MYC* has another enhancer element in its 3'-flanking region (31). Therefore, *MOSPD1* may have additional enhancer region(s) in addition to the one identified here.

In conclusion, we have discovered that *MOSPD1* is a novel target gene of the Wnt signaling pathway in CRC. Further analysis of MOSPD1 function will elucidate the precise molecular mechanism underlying the development and progression of CRC, and may contribute to the development of therapeutic strategies against their invasion and metastasis.

Acknowledgements

The authors would like to thank Ms. Seira Hatakeyama (The University of Tokyo) for their technical assistance.

Funding

This work was supported by the Japan Society for the Promotion of Science, Grant-in-Aid for Scientific Research [grant no. JP20K07563 (K.Y.)].

Availability of data and materials

Gene expression values of human colorectal tumors analyzed during the current study are available in the Gene Expression Omnibus repository under accession number GSE21510 (https://www.ncbi.nlm.nih.gov/geo/query/acc.cgi?acc=GSE21510). The other datasets used and /or analyzed during the current study are available from the corresponding author on reasonable request.

Authors' contributions

The experiments were designed by KY and YF. The experiments were performed by CH, CZ, SN, YI and YT. Data analysis was performed by CH, CZ, KT, TI, YO, SA, YI, GT, YA and DS. CH, CZ, KY and YF confirm the authenticity of all the raw data. The manuscript was written by CH, KY and YF. All authors read and approved the final version of the manuscript.

Ethics approval and consent to participate

This study was approved by the ethical committee of the Institute of Medical Science, The University of Tokyo (approval nos. IMSUT-IRB, 21-14-0806 and 2020-78-0318). All colorectal tumor tissues and corresponding non-cancerous tissues were obtained with written informed consent from the resected specimens of patients who underwent surgery.

Patient consent for publication

Not applicable.

Competing interests

The authors declare that they have no competing interests.

References

1. Clevers H: Wnt/beta-catenin signaling in development and disease. Cell 127: 469-480, 2006.
2. Voloshanenko O, Erdmann G, Dubash TD, Augustin I, Metzig M, Moffa G, Hundsrucker C, Kerr G, Sandmann T, Anchang B, *et al*: Wnt secretion is required to maintain high levels of Wnt activity in colon cancer cells. Nat Commun 4: 2610, 2013.
3. Wang W, Xu L, Liu P, Jairam K, Yin Y, Chen K, Sprengers D, Peppelenbosch MP, Pan Q and Smits R: Blocking wnt secretion reduces growth of hepatocellular carcinoma cell lines mostly independent of β-catenin signaling. Neoplasia 18: 711-723, 2016.
4. Cleary AS, Leonard TL, Gestl SA and Gunther EJ: Tumour cell heterogeneity maintained by cooperating subclones in Wnt-driven mammary cancers. Nature 508: 113-117, 2014.
5. Behrens J, Von Kries JP, Kühl M, Bruhn L, Wedlich D, Grosschedl R and Birchmeier W: Functional interaction of beta-catenin with the transcription factor LEF- 1. Nature 382: 638-642, 1996.
6. He TC, Sparks AB, Rago C, Hermeking H, Zawel L, da Costa LT, Morin PJ, Vogelstein B and Kinzler KW: Identification of c-MYC as a target of the APC pathway. Science 281: 1509-1512, 1998.
7. Tetsu O and McCormick F: Beta-catenin regulates expression of cyclin D1 in colon carcinoma cells. Nature 398: 422-426, 1999.
8. Frietze S, Wang R, Yao L, Tak YG, Ye Z, Gaddis M, Witt H, Farnham PJ and Jin VX: Cell type-specific binding patterns reveal that TCF7L2 can be tethered to the genome by association with GATA3. Genome Biol 13: R52, 2012.
9. Zhu C, Yamaguchi K, Ohsugi T, Terakado Y, Noguchi R, Ikenoue T and Furukawa Y: Identification of FERM domain-containing protein 5 as a novel target of β-catenin/TCF7L2 complex. Cancer Sci 108: 612-619, 2017.
10. Fujita M, Furukawa Y, Tsunoda T, Tanaka T, Ogawa M and Nakamura Y: Up-regulation of the ectodermal-neural cortex 1 (ENC1) gene, a downstream target of the β-catenin/T-cell factor complex, in colorectal carcinomas. Cancer Res 61: 7722-7726, 2001.
11. Miwa N, Furuse M, Tsukita S, Niikawa N, Nakamura Y and Furukawa Y: Involvement of claudin-1 in the beta-catenin/Tcf signaling pathway and its frequent upregulation in human colorectal cancers. Oncol Res 12: 469-476, 2001.
12. Takahashi M, Tsunoda T, Seiki M, Nakamura Y and Furukawa Y: Identification of membrane-type matrix metalloproteinase-1 as a target of the beta-catenin/Tcf4 complex in human colorectal cancers. Oncogene 21: 5861-5867, 2002.
13. Yamaguchi K, Zhu C, Ohsugi T, Yamaguchi Y, Ikenoue T and Furukawa Y: Bidirectional reporter assay using HAL promoter and TOPFLASH improves specificity in high-throughput screening of Wnt inhibitors. Biotechnol Bioeng 114: 2868-2882, 2017.

14. Sandelin A, Alkema W, Engström P, Wasserman WW and Lenhard B: JASPAR: An open-access database for eukaryotic transcription factor binding profiles. Nucleic Acids Res 32: D91-D94, 2004.
15. Yamaguchi K, Yamaguchi R, Takahashi N, Ikenoue T, Fujii T, Shinozaki M, Tsurita G, Hata K, Niida A, Imoto S, *et al*: Overexpression of cohesion establishment factor DSCC1 through E2F in colorectal cancer. PLoS One 9: e85750, 2014.
16. Hagege H, Klous P, Braem C, Splinter E, Dekker J, Cathala G, de Laat W and Forné T: Quantitative analysis of chromosome conformation capture assays (3C-qPCR). Nat Protoc 2: 1722-1733, 2007.
17. Tsukamoto S, Ishikawa T, Iida S, Ishiguro M, Mogushi K, Mizushima H, Uetake H, Tanaka H and Sugihara K: Clinical significance of osteoprotegerin expression in human colorectal cancer. Clin Cancer Clin 17: 2444-2450, 2011.
18. Schatoff EM, Leach BI and Dow LE: Wnt Signaling and colorectal cancer. Curr Colorectal Cancer Rep 13: 101-110, 2017.
19. Takahashi N, Yamaguchi K, Ikenoue T, Fujii T and Furukawa Y: Identification of two Wnt-responsive elements in the intron of RING finger protein 43 (RNF43) Gene. PLoS One 9: e86582, 2014.
20. Thaler R, Rumpler M, Spitzer S, Klaushofer K and Varga F: Mospd1, a new player in mesenchymal versus epidermal cell differentiation. J Cell Physiol 226: 2505-2515, 2011.
21. Klass MR and Hirsh D: Sperm isolation and biochemical analysis of the major sperm protein from caenorhabditis elegans. Dev Biol 84: 299-312, 1981.
22. Sepsenwol S, Ris H and Roberts TM: A unique cytoskeleton associated with crawling in the amoeboid sperm of the nematode, Ascaris suum. J Cell Biol 108: 55-66, 1989.
23. Nelson GA, Roberts TM and Ward S: Caenorhabditis elegans spermatozoan locomotion: Amoeboid movement with almost no actin. J Cell Biol 92: 121-131, 1982.
24. Kara M, Axton RA, Jackson M, Ghaffari S, Buerger K, Watt AJ, Taylor AH, Orr B, Hardy WR, Peault B and Forrester LM: A role for MOSPD1 in mesenchymal stem cell proliferation and differentiation. Stem Cells 33: 3077-3086, 2015.
25. Puiffe ML, Le Page C, Filali-Mouhim A, Zietarska M, Ouellet V, Tonin PN, Chevrette M, Provencher DM and Mes-Masson AM: Characterization of ovarian cancer ascites on cell invasion, proliferation, spheroid formation, and gene expression in an in vitro model of epithelial ovarian cancer. Neoplasia 9: 820-829, 2007.
26. Puisieux A, Brabletz T and Caramel J: Oncogenic roles of EMT-inducing transcription factors. Nat Cell Biol 16: 488-494, 2014.
27. Dancer JY, Henry SP, Bondaruk J, Lee S, Ayala AG, de Crombrugghe B and Czerniak B: Expression of master regulatory genes controlling skeletal development in benign cartilage and bone forming tumors. Hum Pathol 41: 1788-1793, 2010.
28. Groen EJ, Roos A, Muntinghe FL, Enting RH, de Vries J, Kleibeuker JH, Witjes MJH, Links TP and van Beek AP: Extra-intestinal manifestations of familial adenomatous polyposis. Ann Surg Oncol 15: 2439-2450, 2008.
29. Takahashi M, Nakamura Y, Obama K and Furukawa Y: Identification of SP5 as a downstream gene of the beta-catenin/Tcf pathway and its enhanced expression in human colon cancer. Int J Oncol 27: 1483-1487, 2005.
30. Jho EH, Zhang T, Domon C, Joo CK, Freund JN and Costantini F: Wnt/beta-catenin/Tcf signaling induces the transcription of axin2, a negative regulator of the signaling pathway. Mol Cell Biol 22: 1172-1183, 2002.
31. Yochum GS, Cleland R and Goodman RH: A genome-wide screen for beta-catenin binding sites identifies a downstream enhancer element that controls c -myc gene expression. Mol Cell Biol 28: 7368-7379, 2008.